



OPEN Anatomical and anthropometric predictors of femoral and saphenous nerve location for ultrasound guided procedures

Sara Mogedano-Cruz¹, Ignacio Benítez-Chulia¹, Laura González-Fernández¹, Ángel González-de-la-flor¹, Juan Antonio Valera-Calero^{2,3}, Gustavo Plaza-Manzano^{2,3}, Gonzalo Jaén-Crespo¹ & Carlos Romero-Morales¹✉

The accurate identification of peripheral nerves using ultrasound is essential for the safe and effective application of image-guided interventions in pain management. The femoral nerve (FN) and saphenous nerve (SN) are common targets for peripheral nerve invasive techniques, yet their depth and anatomical variability can impact procedural success. The objective was to describe the ultrasound anatomy of the FN and SN in healthy individuals and analyze how anthropometric variables predict its location. Design: A cross-sectional study was conducted in 30 healthy participants. Ultrasound measurements included subcutaneous tissue thickness, nerve depth, and cross-sectional area of the FN and SN. Anthropometric data such as BMI, limb length, and circumference measurements were also recorded. Pearson correlations and hierarchical regression models were used to identify predictors of nerve location. Results: No significant side-to-side differences were found for any variable ($p > 0.05$). Subcutaneous tissue thickness and limb circumference showed strong correlations with nerve depth. The final hierarchical regression model explained 67.0% of the variance in skin-to-FN distance and 82.3% for skin-to-SN distance. Subcutaneous tissue at the inguinal region and mid-thigh, as well as lower limb length and mid-thigh circumference, were significant predictors for FN depth. For the SN, subcutaneous thickness at mid-thigh, mid-thigh circumference, and inguinal subcutaneous tissue were the most relevant predictors. Conclusion: Anthropometric variables, especially subcutaneous tissue thickness and limb circumferences, are reliable predictors of FN and SN depth in healthy subjects. These findings support the use of simple anatomical measures to improve planning and safety in ultrasound-guided procedures.

Keywords Ultrasonography, Diagnostic accuracy studies, Reliability, Femoral nerve, Saphenous nerve

A detailed understanding of the anatomy of peripheral nerves has become an essential tool in clinical practice, both for diagnostic assessment and for the application of image-guided therapeutic interventions. In particular, the development and consolidation of imaging techniques such as musculoskeletal ultrasound have enabled the precise localization of neural structures, supporting the advancement of minimally invasive procedures including nerve blocks, radiofrequency ablations, and peripheral nerve stimulation¹. These approaches are increasingly used in pain management, as they offer safe, effective, and reproducible alternatives for treating various acute and chronic pain syndromes².

Within this context, the femoral and saphenous nerves play a key role in the interventional management of lower limb pain. However, the success of invasive techniques targeting these structures relies heavily on accurate anatomical knowledge and clear, systematic ultrasound identification^{3,4}.

The femoral nerve (FN) is the largest branch of the lumbar plexus, arising from L2–L4 and descending between the psoas major and iliacus muscles beneath the iliac fascia⁵. Below the inguinal ligament, it enters

¹Faculty of Sport Sciences, Universidad Europea de Madrid, Villaviciosa de Odón, Madrid, Spain. ²Department of Physical Therapy, Faculty of Nursing, Physiotherapy and Podiatry, Universidad Complutense de Madrid, 28040 Madrid, Spain. ³Grupo InPhysio, Instituto de Investigación Sanitaria del Hospital Clínico San Carlos (IdISSC), 28040 Madrid, Spain. ✉email: carlos.romero@universidadeuropea.es

the femoral (Scarpa's) triangle, where it typically lies lateral to the femoral artery¹. In ultrasound short-axis views, the FN appears as an oval hyperechoic structure with internal hypoechoic fascicles, situated between the femoral artery and the sartorius muscle⁶. Distal to the inguinal region, the nerve usually divides into anterior and posterior branches, often separated by the lateral circumflex femoral artery^{7,8}.

The anterior division gives rise to sensory branches innervating the anteromedial thigh, and variably, motor branches to the sartorius muscle. It can be identified between the femoral artery and the sartorius muscle⁶. The posterior division provides motor innervation to the quadriceps femoris, an articular branch to the hip, and one sensory branch: the saphenous nerve^{1,8}.

The saphenous nerve (SN), the longest sensory branch of the FN and has a purely sensory function. It supplies the anteromedial, medial, and posteromedial distal thigh, the prepatellar region, the medial leg, and the medial arch of the foot⁹. It courses distally through the adductor (Hunter's) canal^{10,11}, where it is consistently located medial or anteromedial to the femoral artery, beneath the sartorius muscle, and adjacent to the adductor longus and adductor magnus¹². As the SN progresses toward the knee, it separates from the vessels¹³, which facilitates ultrasound visualization, particularly at the mid- and distal-thigh levels. This region is frequently targeted for ultrasound-guided blocks and minimally invasive procedures³.

Effective postoperative pain control in orthopedic and vascular surgery is a key factor in the patient's functional recovery. Surveys have shown that only 46% of hospitals in the United States have dedicated pain management programs, while 77% of surgical patients report postoperative pain, with 61% describing it as moderate to severe¹⁴. In procedures involving the hip, knee, ankle, or vascular structures, adequate analgesia promotes earlier and more efficient rehabilitation, reduces the need for opioid medications, and improves the patient's postoperative quality of life³. Among the most effective analgesic strategies, peripheral nerve blocks have become a fundamental technique for managing postoperative pain. FN blocks are commonly used after femoral fractures or hip surgeries, while SN blocks are employed to manage postoperative knee pain, localized neuralgias, and as analgesic complements in arthroplasties or ligament repairs³. In both cases, accurate nerve localization and careful planning of needle trajectory are critical to optimize clinical outcomes and minimize risks such as direct nerve injury or procedural failure¹⁴.

Previous work has explored the influence of anthropometric characteristics on the depth of lower limb nerves. For example, a study assessing the femoral and sciatic nerves reported significant correlations between nerve depth and parameters such as BMI¹⁵. More recently, an observational study described how age, sex, and BMI affect the anatomical relationships between the femoral nerve and femoral artery¹⁶. However, no previous research has examined the SN in this context or developed multivariable predictive models incorporating multiple anthropometric factors simultaneously. The present study addresses this gap by analysing both FN and SN depth using comprehensive hierarchical regression models to identify accessible predictors of nerve location.

The primary aim of the present study is to describe the ultrasound anatomy of the FN and SN in healthy individuals, focusing on their location, course, depth, and morphological characteristics. Additionally, the study seeks to evaluate the reproducibility of the measurements and explore potential anatomical variations based on anthropometric variables such as sex, age, and body constitution.

Methods

Study design

This cross-sectional observational study was conducted in accordance with the Strengthening the Reporting of Observational Studies in Epidemiology (STROBE) guidelines and checklist. The study protocol received approval from the Ethics Committee of the Universidad Europea de Madrid, and all procedures were performed in line with the principles outlined in the Declaration of Helsinki. Prior to participation, all subjects provided written informed consent and were given a detailed information sheet outlining the scope and purpose of the study.

Participants

30 participants between 18 and 70 years old were recruited between April and May 2025. All participants were healthy volunteers with no current musculoskeletal, neurological, or systemic conditions. Participants were excluded from the study if they were undergoing any treatment that could affect muscle tone, including medical or physiotherapeutic interventions. Additional exclusion criteria included significant asymmetry between lower limbs (defined as ≥ 1 cm difference in limb length or ≥ 2 cm difference in circumference measurements between sides), a history of surgery in the areas where measurements were taken, or neuromuscular diseases that could alter the normal anatomy of the thigh region, such as sarcopenia or amyotrophic lateral sclerosis, among others. Volunteers with specific medical conditions, such as fractures or tumors, as well as pregnant women, were also excluded. Participants were not excluded based on BMI.

Demographic and anthropometric data

The following demographic data were collected: sex (male/female), age (years), height (m), weight (kg), and body mass index (BMI), calculated as weight divided by height squared ($\text{weight}/\text{height}^2$). Height and weight were measured directly by the research team using a calibrated digital scale and stadiometer.

Anthropometric measurements were obtained using a measuring tape (cm). Lower limb length was measured from the anterior superior iliac spine to the lateral malleolus on both sides with the participant in the supine position. Additionally, circumference measurements were recorded at specific anatomical landmarks, including the gluteal fold at the inguinal region and the mid-thigh level. All anthropometric measurements were performed by the same examiner, who had formal training in standardized measurement techniques. Each measurement was taken twice and the mean value was used for analysis. The intra-rater reliability for anthropometric variables was assessed in a subsample of participants and demonstrated excellent repeatability (ICC_{2,1} range: 0.90–0.95).

Ultrasound imaging procedure

Participants included in the study were placed in a supine position with the leg fully extended. All measurements were performed by a single examiner with prior training (6 years) in musculoskeletal ultrasound, using a VScan Air™ (GE Healthcare, Chicago, IL, EE. UU.) wireless ultrasound probe. A linear transducer operating at 3–12 MHz was used for all examinations, and the musculoskeletal-superficial preset was selected as the default imaging mode. Equipment settings—particularly frequency and depth—were individually adjusted for each volunteer to optimize image quality. During the examination, minimal pressure was applied with the probe to avoid compression of the subcutaneous tissue and prevent measurement bias. The ultrasound assessment included analysis of subcutaneous tissue thickness, the distance from the skin to the nerve, and the cross-sectional area (CSA) of the nerve. All ultrasound measurements were performed twice by the same examiner, and the mean value was used for analysis. Intra-rater reliability was assessed in a subsample of participants and demonstrated excellent repeatability for both nerves (FN depth: ICC_{2,1} = 0.92; SN depth: ICC_{2,1} = 0.90).

For the localization of the FN, the ultrasound probe was initially placed over the Scarpa's triangle, using the femoral artery pulse as a primary anatomical landmark. Medial to the artery, the femoral vein was identified. A transverse (short-axis) scan of the nerve was performed to assess the CSA, using the ultrasound device's tracing tool to outline the inner boundary of the hyperechoic nerve edge. As shown in Fig. 1A, the FN was clearly identifiable alongside the femoral artery and vein. Perpendicular measurements were used to assess the subcutaneous tissue thickness and the distance from the skin to the FN (in centimeters), ensuring accurate localization and evaluation. Nerve depth was defined as the perpendicular distance from the skin surface to the superior (superficial) border of the nerve.

For the localization of the SN, the ultrasound probe was positioned transversely on the medial aspect of the mid-thigh, using the course of the saphenous vein as an anatomical reference. The SN was identified within the path of the sartorius muscle. A transverse (short-axis) scan was performed to assess the CSA. As illustrated in Fig. 1B, the ultrasound image clearly reveals the SN near the saphenous vein and surrounding muscular structures. Additionally, calipers were used to measure the subcutaneous tissue thickness and the shortest distance (in centimeters) between the SN and the skin surface.

Statistical analysis

An a priori sample size calculation was performed using GPower 3.1 (University of Düsseldorf, Germany) for multiple linear regression (fixed model, R² deviation from zero). Assuming a medium-to-large effect size ($f^2 = 0.35$), an alpha level of 0.05, a statistical power of 0.80, and up to five predictors, the required minimum sample size was 29 participants. Our final sample of 30 participants therefore exceeded the recommended threshold.

Data analysis was conducted using the JASP software (Jefferys Amazing Statistics Program, Version 0.17, University of Amsterdam, Netherlands. Available at <http://jasp-stats.org>) for Windows. All variables met the assumption of normality according to the Shapiro–Wilk test ($p > 0.05$); therefore, Pearson's correlation coefficients were appropriate for assessing linear associations. After confirming sample homogeneity (using

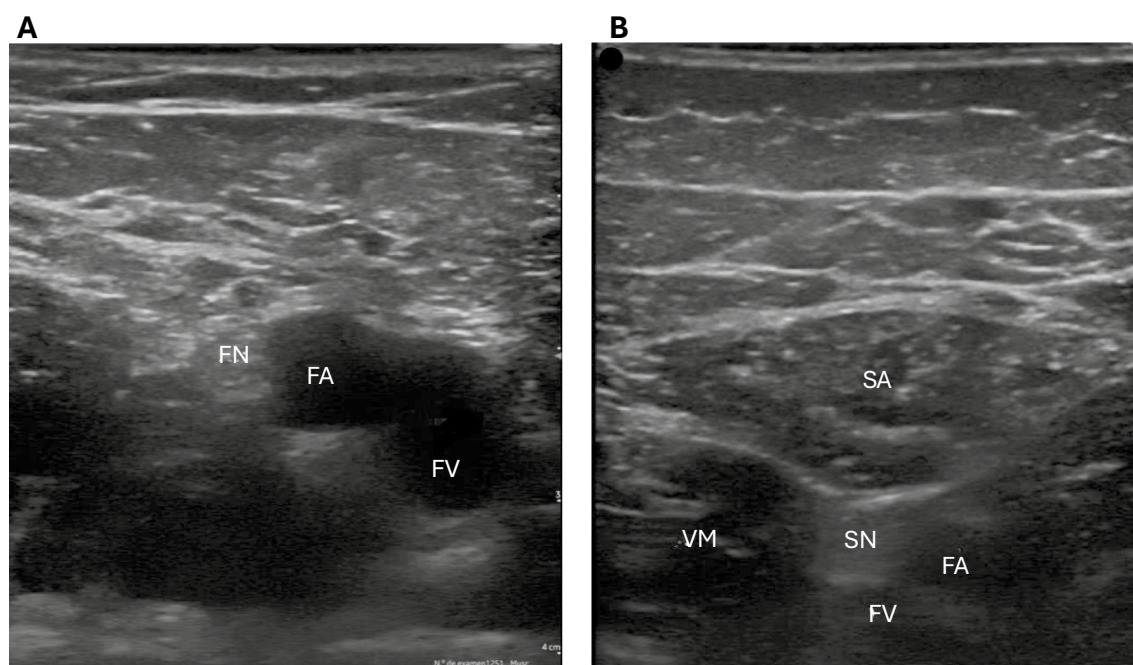


Fig. 1. (A) Femoral nerve alongside the femoral vessels. FN: femoral nerve. FA: femoral artery. FV: femoral vein. (B) Saphenous nerve adjacent to the sartorius muscle. SA: sartorius. VM: vastus medialis. SN: saphenous nerve. FA: femoral artery. FV: femoral vein.

Variable	Mean \pm SD (Min–Max)
Age (years)	36.27 \pm 13.81 (18–67)
Weight (kg)	73.93 \pm 17.91 (42–110)
Height (m)	1.75 \pm 0.11 (1.59–1.96)
BMI (kg/m ²)	23.84 \pm 4.04 (16.61–32.14)

Table 1. Sociodemographic data of the sample (n = 30).

Variable	Total (N = 60)	Left Limb (N = 30)	Right Limb (N = 30)	Mean Difference	p value	Effect Size (Cohen's d)
Subcutaneous tissue in the groin (mm)	0.56 \pm 0.25 (0.21–1.10)	0.60 \pm 0.26 (0.21–1.10)	0.53 \pm 0.24 (0.23–1.00)	0.07 (–0.06, 0.19)	0.292	0.275 (–0.24, 0.78)
Distance from skin to femoral nerve (mm)	1.80 \pm 0.58 (0.83–2.95)	1.82 \pm 0.57 (0.83–2.95)	1.79 \pm 0.60 (0.83–2.95)	0.04 (–0.27, 0.34)	0.817	0.060 (–0.45, 0.57)
Cross-sectional area of the femoral nerve (cm ²)	0.30 \pm 0.03 (0.24–0.39)	0.30 \pm 0.03 (0.24–0.39)	0.29 \pm 0.03 (0.24–0.36)	0.01 (–0.01, 0.02)	0.208	0.329 (–0.18, 0.84)
Subcutaneous tissue in the mid-thigh (mm)	1.57 \pm 0.49 (0.70–2.68)	1.56 \pm 0.50 (0.70–2.68)	1.59 \pm 0.48 (0.70–2.68)	–0.03 (–0.29, 0.22)	0.789	–0.069 (–0.58, 0.44)
Distance from skin to saphenous nerve (mm)	2.91 \pm 0.55 (1.77–4.41)	2.90 \pm 0.52 (1.77–4.41)	2.93 \pm 0.59 (1.77–4.41)	–0.03 (–0.32, 0.26)	0.842	–0.052 (–0.56, 0.46)
Cross-sectional area of the saphenous nerve (cm ²)	0.21 \pm 0.02 (0.16–0.26)	0.21 \pm 0.02 (0.16–0.26)	0.21 \pm 0.03 (0.16–0.26)	–0.00 (–0.01, 0.01)	0.671	–0.110 (–0.62, 0.40)
Inguinal circumference (cm)	59.60 \pm 6.55 (45.00–72.00)	59.60 \pm 6.62 (45.00–72.00)	59.60 \pm 6.59 (45.00–72.00)	0.00 (–3.41, 3.41)	1.000	0.000 (–0.51, 0.51)
Mid-thigh circumference (cm)	50.55 \pm 4.85 (40.00–59.00)	50.47 \pm 4.93 (40.00–59.00)	50.63 \pm 4.86 (40.00–59.00)	–0.17 (–2.70, 2.36)	0.895	–0.034 (–0.54, 0.47)
Leg length (cm)	92.28 \pm 6.97 (79.00–106.00)	92.30 \pm 7.05 (79.00–106.00)	92.27 \pm 7.01 (79.00–106.00)	0.03 (–3.60, 3.67)	0.985	0.005 (–0.50, 0.51)

Table 2. Ultrasound and anthropometric measurements.

Levene's test), independent sample t-tests were performed to examine side-to-side differences in the selected anthropometric and ultrasound variables.

Pearson correlation analyses were conducted to assess the relationships between the various morphometric and nerve distance measurements. Correlation strengths were categorized as follows: values below 0.3 indicated a poor correlation, 0.3 to 0.5 a fair correlation, 0.6 to 0.8 a moderate correlation, and above 0.8 a strong correlation. Variables showing statistically significant associations ($p < 0.05$) were included in the stepwise multiple linear regression models to estimate the proportion of variance explained in the distance from skin to nerve measurements. Multicollinearity among predictors was assessed using Pearson correlation coefficients, with $r > 0.80$ considered indicative of substantial multicollinearity.

Hierarchical regression models were applied to identify significant predictors for distance from skin to femoral nerve (SFD) and distance from skin to saphenous nerve (SSD). The entry criterion for each step in the hierarchical model was set at $p < 0.05$, with adjusted R^2 values reported to reflect the incremental contribution of each added variable in explaining the variance. Model assumptions, including normality, homoscedasticity, and independence of residuals, were tested and confirmed. Linearity of the relationships between predictors and the dependent variables was verified through inspection of partial regression plots and residual-versus-predicted value plots. Residuals were approximately normally distributed (Shapiro–Wilk test, $p > 0.05$), and no significant autocorrelation was observed (Durbin–Watson statistics close to 2.0).

Results

A total of 30 participants (60 limbs) were included in the study. The sample consisted of 17 females (56.7%) and 13 males (43.3%). Exploratory analyses comparing males and females showed no significant sex-related differences in femoral or saphenous nerve depth, nor in the anthropometric variables included in the study (all $p > 0.05$). Therefore, sex was not retained as a predictor in the regression models. The demographic characteristics, including age, weight, height, and BMI are summarized in Table 1.

Between limbs comparisons

Regarding the ultrasound and anthropometric measurements, there were no significant differences between the left and right sides for any of the assessed variables, including subcutaneous tissue in the inguinal region (STI), SFD, cross-sectional area of the femoral nerve (CSA FN), subcutaneous tissue in the mid-thigh (STM), SSD, cross-sectional area of the saphenous nerve (CSA SN), inguinal circumference (IC), mid-thigh circumference (MTC), and lower limb length (LL) ($p > 0.05$ for all comparisons) (Table 2). Since no significant side-to-side differences were found, left and right limb measurements were averaged and the mean value was used for the subsequent correlation and regression analyses.

Variable	BMI	STI	SFD	CSA FN	STM	SSD	CSA SN	IC	MTC
BMI	–								
STI	0.661**	–							
SFD	0.697**	0.744**	–						
CSA FN	0.376*	0.433**	0.418**	–					
STM	0.453*	0.549**	0.613**	0.319*	–				
SSD	0.618**	0.652**	0.703**	0.442**	0.861**	–			
CSA SN	0.633**	0.310*	0.492**	0.501**	0.141	0.260*	–		
IC	0.814**	0.567**	0.606**	0.488**	0.511**	0.674**	0.522**	–	
MTC	0.809**	0.469**	0.543**	0.387**	0.381**	0.580**	0.459**	0.916**	–
LL	0.354	0.354*	0.386**	0.220	-0.089	0.121	0.373**	0.306*	0.209

Table 3. Pearson correlation matrix. BMI: Body Mass Index; STI: Subcutaneous Tissue in the Inguinal Region; SFD: Distance from Skin to Femoral Nerve; CSA FN: Cross-Sectional Area of the Femoral Nerve; STM: Subcutaneous Tissue in the Mid-Thigh; SSD: Distance from Skin to Saphenous Nerve; CSA SN: Cross-Sectional Area of the Saphenous Nerve; IC: Inguinal Circumference; MTC: Mid-Thigh Circumference; LL: Leg Length; $p < 0.05$ (*); $p < 0.01$ (**).

Step	Predictor	B	SE B	95% CI for B	β	t	p	Adjusted R ²
1	STI	1.746	0.206	1.333, 2.158	0.744	8.477	<0.001	0.546
2	STI	1.369	0.231	0.905, 1.832	0.583	5.916	<0.001	0.600
	STM	0.348	0.117	0.113, 0.583	0.292	2.967	0.004	
3	STI	1.001	0.247	0.507, 1.496	0.427	4.059	<0.001	0.651
	STM	0.479	0.118	0.244, 0.715	0.403	4.077	<0.001	
	LL	0.023	0.007	0.008, 0.037	0.271	3.074	0.003	
4	STI	0.876	0.248	0.380, 1.372	0.373	3.539	<0.001	0.670
	STM	0.431	0.117	0.197, 0.665	0.362	3.695	<0.001	
	LL	0.021	0.007	0.006, 0.035	0.249	2.883	0.006	
	MTC	0.021	0.010	0.001, 0.042	0.178	2.056	0.045	

Table 4. Regression model for distance from skin to femoral nerve. BMI: Body Mass Index; STI: Subcutaneous Tissue in the Inguinal Region; SFD: Distance from Skin to Femoral Nerve; STM: Subcutaneous Tissue in the Mid-Thigh; MTC: Mid-Thigh Circumference; LL: Leg Length; B: Unstandardized Coefficient; SE B: Standard Error of B; 95% CI for B: 95% Confidence Interval for B; β : Standardized Coefficient; t: t-value; p: p-value; Adjusted R²: Adjusted R-Squared.

Correlation analysis

Correlation analysis (Table 3) revealed several significant relationships among the measured variables. Notably, BMI showed strong positive correlations with IC ($r = 0.814$, $p < 0.01$) and MTC ($r = 0.809$, $p < 0.01$), as well as moderate positive correlations with STI ($r = 0.661$, $p < 0.01$), SFD ($r = 0.697$, $p < 0.01$), and SSD ($r = 0.618$, $p < 0.01$).

STI also correlated strongly with SFD ($r = 0.744$, $p < 0.01$) and moderately with CSA FN ($r = 0.433$, $p < 0.01$). Similarly, SFD showed strong positive correlations with SSD ($r = 0.703$, $p < 0.01$) and moderate correlations with STM ($r = 0.613$, $p < 0.01$).

Interestingly, CSA SN area was moderately correlated with IC ($r = 0.522$, $p < 0.01$) and MTC ($r = 0.459$, $p < 0.01$), but not significantly correlated with STM ($r = 0.141$, $p = 0.282$).

No significant correlations were found between LL and most other variables, except for weak positive correlations with MTC ($r = 0.306$, $p < 0.05$) and CSA SN ($r = 0.373$, $p < 0.01$).

Hierarchical regression model of the distance from the skin to the femoral nerve

A hierarchical linear regression was conducted to identify significant predictors of the SFD (Table 4).

Step 1 included only STI as a predictor, which explained 54.6% of the variance in the dependent variable (adjusted R² = 0.546, $p < 0.001$). The unstandardized coefficient for STI was 1.746 (95% CI 1.333, 2.158), indicating a strong positive association ($\beta = 0.744$, $t = 8.477$, $p < 0.001$). Step 2 added STM, which significantly improved the model fit (adjusted R² = 0.600). STI remained a significant predictor ($B = 1.369$, 95% CI 0.905, 1.832, $\beta = 0.583$, $p < 0.001$), while STM also contributed significantly ($B = 0.348$, 95% CI 0.113, 0.583, $\beta = 0.292$, $p = 0.004$).

Step 3 further included LL, increasing the adjusted R² to 0.651. In this step, STI ($B = 1.001$, 95% CI 0.507, 1.496, $\beta = 0.427$, $p < 0.001$), STM ($B = 0.479$, 95% CI 0.244, 0.715, $\beta = 0.403$, $p < 0.001$), and LL ($B = 0.023$, 95% CI 0.008, 0.037, $\beta = 0.271$, $p = 0.003$) all emerged as significant predictors. Step 4 included MTC as an additional predictor, resulting in an adjusted R² of 0.670. In this final model, STI ($B = 0.876$, 95% CI 0.380, 1.372, $\beta = 0.373$, $p < 0.001$), STM ($B = 0.431$, 95% CI 0.197, 0.665, $\beta = 0.362$, $p < 0.001$), LL ($B = 0.021$, 95% CI 0.006, 0.035, $\beta = 0.249$,

Step	Predictor	B	SE B	95% CI for B	β	t	p	Adjusted R ²
1	STM	0.976	0.076	0.824, 1.127	0.861	12.876	<0.001	0.736
2	STM	0.848	0.070	0.708, 0.988	0.748	12.148	<0.001	0.809
	MTC	0.033	0.007	0.019, 0.047	0.295	4.789	<0.001	
3	STM	0.767	0.075	0.616, 0.917	0.676	10.180	<0.001	0.823
	MTC	0.028	0.007	0.013, 0.042	0.244	3.890	<0.001	
	STI	0.372	0.155	0.061, 0.683	0.166	2.395	0.020	

Table 5. Regression model for distance from skin to saphenous nerve. BMI: Body Mass Index; STI: Subcutaneous Tissue in the Inguinal Region; STM: Subcutaneous Tissue in the Mid-Thigh; MTC: Mid-Thigh Circumference; B: Unstandardized Coefficient; SE B: Standard Error of B; 95% CI for B: 95% Confidence Interval for B; β : Standardized Coefficient; t: t value; p: p value; Adjusted R²: Adjusted R-Squared; p < 0.05 (*); p < 0.01 (**).

p = 0.006), and MTC (B = 0.021, 95% CI 0.001, 0.042, β = 0.178, p = 0.045) were all significant contributors to the model.

The assumptions of normality, homoscedasticity, and independence of residuals were verified. Residuals were approximately normally distributed, as indicated by the non-significant Shapiro–Wilk test (p > 0.05), and no substantial multicollinearity was observed, with variance inflation factors (VIFs) for all predictors below 2.0. The Durbin–Watson statistic indicated no significant autocorrelation in the residuals (Durbin–Watson = 1.957).

Hierarchical regression model of the distance from the skin to the saphenous nerve

A hierarchical linear regression was performed to identify key predictors of the SSD (Table 5).

In Step 1, STM was included as the sole predictor, explaining 73.6% of the variance in the dependent variable (adjusted R² = 0.736, p < 0.001). The unstandardized coefficient for STM was 0.976 (95% CI 0.824, 1.127), indicating a strong positive relationship (β = 0.861, t = 12.876, p < 0.001). Step 2 incorporated MTC, which significantly enhanced the model's predictive power, increasing the adjusted R² to 0.809. In this model, STM remained a significant predictor (B = 0.848, 95% CI 0.708, 0.988, β = 0.748, p < 0.001), while MTC also showed a substantial contribution (B = 0.033, 95% CI 0.019, 0.047, β = 0.295, p < 0.001).

In Step 3, STI, was added, further improving the model fit, resulting in an adjusted R² of 0.823. In this final model, STM (B = 0.767, 95% CI 0.616, 0.917, β = 0.676, p < 0.001), MTC (B = 0.028, 95% CI 0.013, 0.042, β = 0.244, p < 0.001), and STI (B = 0.372, 95% CI 0.061, 0.683, β = 0.166, p = 0.020) all emerged as significant predictors.

Model assumptions, including normality, homoscedasticity, and independence of residuals, were tested and confirmed. Residuals displayed a roughly normal distribution (Shapiro–Wilk test, p > 0.05), no evidence of multicollinearity was detected (all VIFs < 2.0), and no significant autocorrelation was observed (Durbin–Watson = 2.499).

Discussion

This study is among the first to explore the relationship between anatomical parameters of the FN and SN, assessed via ultrasound, and easily obtainable anthropometric variables in a healthy population. The findings demonstrate that subcutaneous tissue thickness and limb circumference measurements are reliable predictors of nerve depth, particularly in the inguinal and mid-thigh regions. The predictive models accounted for a substantial proportion of the variance in skin-to-nerve distance, with adjusted R² values of 0.670 for the FN and 0.823 for the SN.

Previous research has examined the influence of anthropometric variables on peripheral nerve depth, but these studies have focused mainly on other nerves or relied on simple bivariate associations. Importantly, no prior work has developed multivariable predictive models for femoral and saphenous nerve depth or examined the SN specifically in relation to anthropometry. Our study addresses this gap by identifying the most relevant anatomical predictors using hierarchical regression models.

These results align with previous investigations involving the median nerve, where BMI and limb circumference have been identified as consistent predictors of nerve depth¹⁷. Similarly, a recent study on the sciatic nerve found that basic anthropometric variables—such as sex, BMI, and thigh circumference—were significantly associated with nerve depth¹⁸. Collectively, these findings underscore the clinical utility of incorporating anthropometric measurements to anticipate the depth of neurovascular structures, thereby supporting more accurate planning of invasive procedures and reducing the risk of accidental puncture.

Notably, STI emerged as the strongest predictor of FN depth across all steps of the regression model. When additional predictors were introduced—such as STM, LL, and MTC—the model's predictive power improved incrementally. Similarly, the most robust predictor of SN depth was STM, followed by MTC and STI. These findings are anatomically plausible, as greater subcutaneous adipose tissue in these regions naturally increases the distance between the skin and the underlying nerve¹⁹.

These findings are consistent with previous anatomical and ultrasound-based studies describing the predictable course and depth of the femoral and saphenous nerves. For the FN, prior work has shown that subcutaneous tissue thickness and thigh circumference are associated with greater nerve depth^{15,18}, which aligns with our identification of inguinal and mid-thigh adiposity as primary predictors. Similarly, cadaveric and imaging studies of the SN have demonstrated stable medial positioning within the adductor canal, with

depth variations influenced by regional adipose tissue⁹—findings that parallel the strong effect of mid-thigh subcutaneous thickness observed in our model. These convergences reinforce the anatomical basis of the predictive relationships identified in our study.

It is worth noting that, while nerve depth was strongly influenced by anthropometric variables, the CSA of the nerves proved less predictable. Although moderate correlations between CSA and circumference measurements were observed, no strong associations were found with subcutaneous thickness or BMI. This suggests that factors such as neural mobility, physical activity level, or local vascular dynamics may exert greater influence on CSA than general body composition²⁰.

The clinical relevance of these findings lies in their potential to enhance the safety and precision of invasive procedures, where accurate knowledge of nerve depth is essential to minimize complications and ensure correct targeting²¹. The data support the future development of practical tools—such as anthropometric reference charts or mobile applications—that estimate nerve depth based on subcutaneous thickness and circumference measurements.

However, several limitations should be acknowledged. This study was conducted in a healthy population, limiting the generalizability of its results to individuals with musculoskeletal or systemic conditions, where anatomical alterations may affect nerve positioning. Furthermore, although both lower limbs were assessed, all participants were asymptomatic and presented a relatively narrow BMI range, potentially underestimating interindividual variability. Additional research is needed to validate these models in broader and more heterogeneous populations, including individuals with obesity, muscle hypertrophy, or peripheral neuropathies.

Another limitation lies in the absence of interobserver reliability assessment, as all ultrasound measurements were performed by a single examiner. This lack of reproducibility testing restricts the external validity of the proposed model and its clinical applicability in settings involving multiple operators. Additionally, given the modest sample size and the number of predictors included in the regression models, the possibility of overfitting or instability in the regression coefficients cannot be completely ruled out.

Future studies should also consider the inclusion of complementary variables such as muscle mass, fascial thickness, and regional biomechanical dynamics. Integrating these parameters may enhance the explanatory capacity of predictive models and support the development of more precise clinical guidelines for interventions targeting the FN and SN.

Conclusions

This study demonstrates that subcutaneous tissue thickness and limb circumference are key predictors of the depth of the FN and SN at the inguinal and mid-thigh levels. The regression models developed showed a strong ability to estimate nerve depth using simple anthropometric measurements, which may significantly enhance the safety and precision of invasive procedures. These findings highlight the clinical relevance of incorporating accessible metrics for nerve localization, potentially reducing the risk of accidental puncture and improving the efficacy of therapeutic interventions.

Data availability

Data materials could be shared under formal request to the corresponding author.

Received: 24 June 2025; Accepted: 3 December 2025

Published online: 14 December 2025

References

- Fenech, M., Roche, B. & Boyle, J. Ultrasound imaging of the femoral and saphenous nerves. *Australas J. Ultrasound Med.* **27**(4), 229–241 (2024).
- Fonkoue, L. et al. Anatomical study of the descending genicular artery and implications for image-guided interventions for knee pain. *Clin. Anat.* **34**(4), 634–643 (2021).
- Niyonkuru, E., Iqbal, M. A., Zeng, R., Zhang, X., & Ma P. Nerve Blocks for Post-Surgical Pain Management: A Narrative Review of Current Research. *J. Pain Res.* 2024;
- Bowley, M. P. & Doughty, C. T. Entrapment neuropathies of the lower extremity. *Med. Clin. North Am.* **103**(2), 371–382 (2019).
- Moore, A. E. & Stringer, M. D. Iatrogenic femoral nerve injury: A systematic review. *Surg. Radiol. Anat.* **33**(8), 649–658 (2011).
- Yeo, Y., Son, H. M. & Lee, S. M. ultrasound imaging of cutaneous innervations of the lower extremity. *J. Ultrasound Med.* **39**(7), 1421–1433 (2020).
- De Maeseener, M. et al. Normal anatomy and compression areas of nerves of the foot and ankle: US and MR imaging with anatomic correlation. *Radiogr. Rev. Publ. Radiol. Soc. North Am.* **35**(5), 1469–1482 (2015).
- Orebaugh, S. L. The femoral nerve and its relationship to the lateral circumflex femoral artery. *Anesth. Analg.* **102**(6), 1859–1862 (2006).
- Burckett-St Laurant, D. et al. The nerves of the adductor canal and the innervation of the knee: An anatomic study. *Reg. Anesth. Pain Med.* **41**(3), 321–327 (2016).
- Johnston, D. F., Black, N. D., Cowden, R., Turbitt, L. & Taylor, S. Spread of dye injectate in the distal femoral triangle versus the distal adductor canal: A cadaveric study. *Reg. Anesth. Pain Med.* **44**(1), 39–45 (2019).
- Ghosh, A. & Chaudhury, S. Morphology of saphenous nerve in cadavers: A guide to saphenous block and surgical interventions. *Anat. Cell Biol.* **52**(3), 262–268 (2019).
- Horn, J. L., Pitsch, T., Salinas, F. & Benninger, B. Anatomic basis to the ultrasound-guided approach for saphenous nerve blockade. *Reg. Anesth. Pain Med.* **34**(5), 486–489 (2009).
- Le Corroller, T., Lagier, A., Pirro, N. & Champsaur, P. Anatomical study of the infrapatellar branch of the saphenous nerve using ultrasonography. *Muscle Nerve.* **44**(1), 50–54 (2011).
- Ilfeld, B. M. et al. Ultrasound-guided percutaneous peripheral nerve stimulation for analgesia following total knee arthroplasty: A prospective feasibility study. *J. Orthop. Surg. Res.* **12**(1), 4 (2017).
- Garkoti, R., Sethi, A. K., Tyagi, A., Moha, M. & Agarwal, D. Depth of femoral and sciatic nerves and its correlation with anthropometric parameters. *J. Anaesthesiol. Clin. Pharmacol.* **25**(1), 59–62 (2009).

16. Shaji S, Thomas Vaidyan KP, Jose S, Godwin A, Rahman M, Mehta P, Sayedkazmi AH, Greiss HFW, Nadhari MMY AO. Impact of age, sex and body mass index on anatomical variations of the femoral nerve in relation to the femoral artery: Implications for ultrasound-guided femoral nerve blocks—An observational study. *Int J Med Sci Clinical Res Rev.* 2024;
17. Karadağ, Y. S. et al. Severity of carpal tunnel syndrome assessed with high frequency ultrasonography. *Rheumatol. Int.* **30**(6), 761–765 (2010).
18. Minguez-Esteban, I. et al. Prediction model for sciatic nerve procedures: A cross-sectional study. *J. Clin. Med.* **13**(24), 7851 (2024).
19. Dhagat, P. K., Jain, M. & Farooq, A. MRI evaluation of soft tissue vascular malformations. *Indian J. Radiol. Imaging.* **30**(02), 184–189 (2020).
20. Massy-Westropp, N., Grimmer, K. & Bain, G. The effect of a standard activity on the size of the median nerve as determined by ultrasound visualization. *J. Hand Surg. Am.* **26**(4), 649–654 (2001).
21. Potter, C. L., Cairns, M. C. & Stokes, M. Use of ultrasound imaging by physiotherapists: A pilot study to survey use, skills and training. *Man. Ther.* **17**(1), 39–46 (2012).

Author contributions

CRediT authorship contributions Sara Mogedago-Cruz: Conceptualization, Investigation, Data curation, Formal analysis, Writing—original draft. Ignacio Benítez-Chuliá: Methodology, Software, Validation, Visualization. Laura González-Fernández: Investigation, Resources, Writing—review & editing. Ángel González-de-la-Flor: Supervision, Project administration, Writing—review & editing. Juan Antonio Valera-Calero: Methodology, Formal analysis, Writing—review & editing. Gustavo Plaza-Manzano: Funding acquisition, Supervision, Writing—review & editing. Gonzalo Jaén-Crespo: Writing—review and editing. Carlos Romero-Morales: Conceptualization, Supervision, Project administration, Writing—review & editing.

Funding

This project was funded through a competitive call, specifically the 5th Call for Research Grants awarded by Ilustre Colegio Profesional de Fisioterapeutas de la Comunidad de Madrid.

Declarations

Competing interests

The authors declare no competing interests.

Ethics approval and consent to participate

The study protocol received approval from the Ethics Committee of the Universidad Europea de Madrid, and all procedures were performed in line with the principles outlined in the Declaration of Helsinki. Prior to participation, all subjects provided written informed consent and were given a detailed information sheet outlining the scope and purpose of the study.

Additional information

Correspondence and requests for materials should be addressed to C.R.-M.

Reprints and permissions information is available at www.nature.com/reprints.

Publisher's note Springer Nature remains neutral with regard to jurisdictional claims in published maps and institutional affiliations.

Open Access This article is licensed under a Creative Commons Attribution-NonCommercial-NoDerivatives 4.0 International License, which permits any non-commercial use, sharing, distribution and reproduction in any medium or format, as long as you give appropriate credit to the original author(s) and the source, provide a link to the Creative Commons licence, and indicate if you modified the licensed material. You do not have permission under this licence to share adapted material derived from this article or parts of it. The images or other third party material in this article are included in the article's Creative Commons licence, unless indicated otherwise in a credit line to the material. If material is not included in the article's Creative Commons licence and your intended use is not permitted by statutory regulation or exceeds the permitted use, you will need to obtain permission directly from the copyright holder. To view a copy of this licence, visit <http://creativecommons.org/licenses/by-nc-nd/4.0/>.

© The Author(s) 2025